On Thermal Instabilities in a Viscoelastic Fluid Subject to Internal Heat Generation

Donna M. G. Comissiong, Tyrone D. Dass, Harold Ramkissoon and Alana R. Sankar

Abstract—The Bénard-Marangoni thermal instability problem for a viscoelastic Jeffreys' fluid layer with internal heat generation is investigated. The fluid layer is bounded above by a realistic free deformable surface and by a plane surface below. Our analysis shows that while the internal heat generation and the relaxation time both destabilize the fluid layer, its stability may be enhanced by an increased retardation time.

Keywords—Viscoelastic fluid, Jeffreys' model, Maxwell model, internal heat generation, retardation time, relaxation time.

I. INTRODUCTION

THE phenomenon of thermal convection was first recognised by Count Rumford in 1797 and James Thomson in 1882 but the earliest set of experiments to demonstrate the onset of thermal instability in fluid was conducted by Bénard in 1900. Bénard exhibited the spontaneous formation of cells in a layer of fluid heated from below [1]. In 1916, Lord Rayleigh being motivated by the work of Bénard, went on to lay the theoretical foundation for the study of convective instability [2]. Scores of papers on thermal convection then followed his first paper. However in 1958, Pearson was the first to neglect the previous explanation of buoyancy and provide a new explanation for the instability in a thin fluid layer based on a surface-tension driven convection [3]. The instability caused by buoyancy was referred to as the Rayleigh-Bénard effect while the term Marangoni instability was used for surface-tension driven convection.

The term Bénard-Marangoni instability began to be used after Nield discovered the mutual influence of both buoyancy and surface-tension driven forces on the stability limit of a fluid [4]. This led to numerous studies being done on Bénard-Marangoni problems worldwide. However, these studies did not examine the possibility of oscillatory instabilities. It was Benguria and Depassier who first studied the existence of oscillatory instabilities in the combined Bénard-Marangoni problem for a Boussinesq fluid bounded above by a free deformable surface [5]. This work was studied numerically by Pérez-García and Carneiro who found examples of situations in which there was competition between a steady and an oscillatory mode and between two oscillatory modes at the onset of convection when the layer was heated from above [6]. A numerical study of the stability of a viscoelastic fluid layer bounded above by a free deformable surface was later done by Ramkissoon et al. [7].

D. M. G. Comissiong, T. D. Dass, H. Ramkissoon and A. R. Sankar are with the Department of Mathematics and Statistics, The University of the West Indies, St. Augustine, Trinidad and Tobago. e-mail for correspondence: Donna.Comissiong@sta.uwi.edu

Research has also been conducted with the consideration of internal heat generation in the fluid undergoing the Bénard-Marangoni convection effect. Sparrow, Goldstein and Johnson and Roberts analysed the thermal instability in a horizontal fluid layer with the nonlinear temperature distribution which was created by an internal heat generation [8]. The study was extended to examine the fluid in a porous medium by several authors (see for example [9], [10] and [11]). Char and Chiang performed a stability analysis of this problem with a deformable surface [12]. This knowledge can be applied to a number of engineering problems like oil extraction from porous media, energy storage in molten salts, crystal growth in space and chemical engineering of paints, colloids and detergents. Char, Chiang and Jou also did an oscillatory instability analysis of Bénard-Marangoni convection in a rotating fluid with internal heat generation [13]. The stabilization of thermocapillary instability in a fluid layer with an internal heat source was examined by Hashim, Othman and Kechil [14]. Nanjundappa et al. researched the effect of internal heat generation on the onset of Brinkman-Bénard convection in a ferrofluid saturated porous layer [15]. The free convection boundary layer flow of a viscoelastic fluid in the presence of heat generation was recently investigated by Abdul, Mohammed and Sharidan [16]. Here, the problem of free convection boundary layer flow of viscoelastic fluid past a horizontal circular cylinder with the constant temperature in the presence of heat generation was examined.

We consider the onset of overstability in a layer of Jeffreys' viscoelastic fluid with a free deformable upper surface and a lower plane surface when subjected to internal heat generation. When the retardation time is set to zero, we obtain the results for the simpler Maxwell viscoelastic model. When the relaxation and retardation times are both taken to be zero, we recover the results for a Newtonian fluid layer with a free deformable upper surface and a lower plane surface when subjected to internal heat generation. Our goal is to determine how the internal heat generation moderates the impact of the relaxation and retardation times on the onset of overstability.

II. GOVERNING EQUATIONS

A horizontal layer of viscoelastic fluid initially at rest between $z = 0$ and $z = d$ acted upon a gravitational field $\mathbf{g} = -g\,\hat{z}$ and subjected to internal heat generation, q, is used. The lower surface is plane (either rigid or stress-free) and a perfect thermal conductor while the upper surface is free, deformable and in contact with an ambient gas which exerts a constant pressure p_a on it. When motion occurrs, the

World Academy of Science, Engineering and Technology
International Journal of Mathematical and Computational Sciences
Vol:5, No:8, 2011

free surface is deformed. The Boussinesq approximation is assumed so that the governing equations of the fluid are

$$\nabla.\mathbf{v} = 0, \qquad (1)$$

$$\rho_0 \frac{d\mathbf{v}}{dt} = -\nabla p + \mathbf{g}\rho + \nabla \cdot \tau, \qquad (2)$$

$$\frac{dT}{dt} = \kappa\nabla^2 T + q, \qquad (3)$$

$$\rho = \rho_0[1 - \alpha(T - T_0)], \qquad (4)$$

$$\xi = \xi_0 - \xi(T - T_0), \qquad (5)$$

while the constituive equation for the viscoelastic fluid is

$$\left(1 + \lambda_1\frac{\partial}{\partial t}\right)\tau = \left(1 + \lambda_2\frac{\partial}{\partial t}\right)\left[\nabla\mathbf{v} + (\nabla\mathbf{v})^{\mathbf{T}}\right],$$

with the convective derivative

$$\frac{d}{dt} = \frac{\partial}{\partial t} + \mathbf{v}.\nabla$$

Here p, T, ρ, τ, ξ and $\mathbf{v}$ denote the pressure, temperature, density, surface tension, the extra-stress tensor and fluid velocity respectively. The quantities ρ_0, ξ_0 and T_0 are reference values and κ, α, γ, λ_1, λ_2, μ and q are fluid constants representing thermal diffusivity, thermal expansion coefficient, rate of change of surface tension with temperature, the relaxation time, the retardation time, viscosity and internal heat generation. Motion is restricted to two dimensions so that $\mathbf{v} = (u, 0, w)$.

To analyse the boundary conditions on the more complex upper surface $z = 1 + \eta$, the unit normal and tangential vectors are considered

$$\mathbf{n} = \frac{\left(-\frac{\partial\eta}{\partial x}, 0, 1\right)}{N}, \qquad (6)$$

$$\mathbf{t} = \frac{\left(1, 0, \frac{\partial\eta}{\partial x}\right)}{N}, \qquad (7)$$

where

$$N = \sqrt{1 + \left(\frac{\partial\eta}{\partial x}\right)^2}.$$

The kinematic stress conditions at the surface are

$$w = \frac{\partial\eta}{\partial t} + u\frac{\partial\eta}{\partial x}, \qquad (8)$$

$$(S''_{ij} - S'_{ij})n_j = -\frac{\xi}{N^3}\frac{\partial^2\eta}{\partial x^2}n_i - \xi_{,k}t_k t_i, \qquad (9)$$

where $''$ and $'$ represent the air and fluids regions respectively and

$$S_{ij} = -p\delta_{ij} + \tau_{ij}.$$

Note that equation (9) can also be written as:

$$(p - p_a)\delta_{ij}n_j - \tau_{ij}n_j = -\frac{\xi}{N^3}\frac{\partial^2\eta}{\partial x^2}n_i - \xi_{,k}t_k t_i.$$

The heat flux equation is given as

$$\kappa\nabla T'.\hat{\mathbf{n}} + hT' = 0$$

where h is the convective heat transfer coefficient (also known as the film coefficient) and

$$T' = T - T_0.$$

These equations are linearized around the static solution and all perturbations are assumed to evolve in time as $e^{\lambda t}$ and in the horizontal variable as e^{iax}. The equations for the perturbations reduce to:

$$\left(D^2 - a^2\right)\left[D^2 - a^2 - \frac{\lambda(1 + \lambda L_1)}{\sigma(1 + \lambda L_2)}\right]\psi(z)$$
$$= iaR\left(\theta(z)\right)\frac{(1 + \lambda L_1)}{(1 + \lambda L_2)}, \qquad (10)$$

$$\left(D^2 - a^2 - \lambda\right)\theta(z) = (1 - Q)\,ia\psi(z), \qquad (11)$$

where $\theta(z)$ is the amplitude of the temperature perturbation, $\psi(z)$ is the amplitude of the streamfunction such that $\psi(x, z, t)$, $\mathbf{v} = (\psi_z, 0, -\psi_x)$, and D is the derivative with respect to the vertical variable z.

The linearized boundary conditions on the upper surface $z = 1 + \eta$ are

$$\lambda\left[D^2 - 3a^2 - \frac{\lambda(1 + \lambda L_1)}{\sigma(1 + \lambda L_2)}\right]D\psi$$
$$-a^2\frac{(1 + \lambda L_1)}{(1 + \lambda L_2)}\left(\sigma G + \frac{a^2}{C}\right)\psi = 0, \qquad (12)$$

$$(D^2 + a^2)\psi - \left[\frac{R\Gamma(1 + Q)}{\left(\sigma G + \frac{a^2}{C}\right)}\right]\left[\begin{array}{c} D^2 - 3a^2 \\ -\frac{\lambda(1 + \lambda L_1)}{\sigma(1 + \lambda L_2)} \end{array}\right]D\psi$$
$$+ia\frac{(1 + \lambda L_1)}{(1 + \lambda L_2)}R\Gamma\theta = 0, \qquad (13)$$

$$D\theta + B_i\left[\theta + \frac{ia\psi}{\lambda}(1 + Q)\right] = 0. \qquad (14)$$

The boundary conditions on the lower surface $z = 0$ are

$$\psi = D\psi = \theta = 0, \qquad (15)$$

if the surface was rigid with no slip and

$$\psi = D^2\psi = \theta = 0, \qquad (16)$$

if it is stress-free. For the purpose of our analysis, we define the following dimensionless variables:

The Prandtl number, $\sigma = \frac{\nu}{\kappa}$ where $\nu = \frac{\mu}{\rho_0}$.

The Rayleigh number, $R = \frac{g\alpha d^3\Delta T}{\kappa\nu}$.

The Capillary number, $C = \frac{\mu\kappa}{\xi_0 d}$.

The Galileo number, $G = \frac{gd^3}{\nu^2}$.

Internal heating, $Q = \frac{qd^2}{2\kappa\Delta T}$.

The non-dimensional relaxation time, $L_1 = \frac{\lambda_1\kappa}{d^2}$.

World Academy of Science, Engineering and Technology
International Journal of Mathematical and Computational Sciences
Vol:5, No:8, 2011

The non-dimensional retardation time, $L_2 = \dfrac{\lambda_2 \kappa}{d^2}$.

The Biot number, $B_i = \dfrac{hd}{\kappa}$.

The Marangoni number, $M = \Gamma R$,

where $\Gamma = \dfrac{\gamma}{\rho_0 g \alpha d^2}$.

Equations (10) and (11) subject to boundary conditions (12) - (15) constitute the problem to be solved for a rigid lower surface. Note that if $L_1 = L_2$ and $Q = 0$, the Newtonian model with no internal heat generation studied by Benguria et al. [5] is recovered, while if we set $L_2 = 0$ and $Q = 0$, we obtain the results for the Maxwell model with no internal heat generation studied by Ramkissoon et al. [7].

Next, the temperature variable is eliminated to yield an equation for ψ

$$\psi \left\{ \begin{array}{l} \left(D^2 - a^2\right)\left(D^2 - a^2 - \lambda\right) \\ \cdot \left[D^2 - a^2 - \dfrac{\lambda\left(1 + \lambda L_1\right)}{\sigma\left(1 + \lambda L_2\right)}\right] \\ + a^2 R\left(1 - Q\right)\left(\dfrac{1 + \lambda L_1}{1 + \lambda L_2}\right) \end{array} \right\} = 0, \qquad (17)$$

subject to the following boundary conditions on $z = 1$

$$\left(D^2 - a^2\right)\left[D^2 - a^2 - \dfrac{\lambda(1 + \lambda L_1)}{\sigma(1 + \lambda L_2)}\right] D\psi$$
$$+ B_i \left\{ \begin{array}{l} \left(D^2 - a^2\right)\left[D^2 - a^2 - \dfrac{\lambda(1 + \lambda L_1)}{\sigma(1 + \lambda L_2)}\right] \\ - \dfrac{Ra^2\left(1 + Q\right)\dfrac{(1 + \lambda L_1)}{(1 + \lambda L_2)}}{\lambda} \end{array} \right\} = 0, \quad (18)$$

$$\lambda\left[D^2 - 3a^2 - \dfrac{\lambda(1 + \lambda L_1)}{\sigma(1 + \lambda L_2)}\right] D\psi$$
$$- a^2 \dfrac{(1 + \lambda L_1)}{(1 + \lambda L_2)}\left(\sigma G + \dfrac{a^2}{C}\right)\psi = 0, \qquad (19)$$

$$\left(D^2 + a^2\right)\psi - \left[\dfrac{\Gamma R\left(1 + Q\right)}{\left(\sigma G + \dfrac{a^2}{C}\right)}\right]\left[\begin{array}{c} D^2 - 3a^2 \\ - \dfrac{\lambda(1 + \lambda L_1)}{\sigma(1 + \lambda L_2)} \end{array}\right] D\psi$$
$$+ \Gamma\left(D^2 - a^2\right)\left[D^2 - a^2 - \dfrac{\lambda(1 + \lambda L_1)}{\sigma(1 + \lambda L_2)}\right]\psi = 0. \qquad (20)$$

On the bottom surface, at $z = 0$,

$$\left(D^2 - a^2\right)\left[D^2 - a^2 - \dfrac{\lambda(1 + \lambda L_1)}{\sigma(1 + \lambda L_2)}\right]\psi = 0, \qquad (21)$$

and either

$$\psi = D\psi = \theta = 0 \qquad (22)$$

for a rigid surface or

$$\psi = D^2\psi = \theta = 0 \qquad (23)$$

for a stress free plane surface.

The solution for ψ may be written as

$$\psi = \sum_{i=1}^{3}\left[A_i\,sinh(\alpha_i z) + B_i\,cosh(\alpha_i z)\right], \qquad (24)$$

where the α_i's are the three different roots of

$$\left(\alpha^2 - a^2\right)\left(\alpha^2 - a^2 - \lambda\right)\left[\alpha^2 - a^2 - \dfrac{\lambda(1 + \lambda L_1)}{\sigma(1 + \lambda L_2)}\right]$$
$$+ a^2 R\left(1 - Q\right)\dfrac{(1 + \lambda L_1)}{(1 + \lambda L_2)} = 0. \qquad (25)$$

Substituing for ψ into equations (18) - (22), provided six homogeneous equations to determine the coefficients A_i and B_i. A non-trivial solution of the system arose when the determinant of the coefficients vanished. This generates the characteristic equation from which the eigenvalues λ and R may be obtained. Considering equations (17) - (21) and (23) it can be shown that the determinant can be written as

$$D_f = [grh], \qquad (26)$$

where $[grh]$ denotes the box product $\mathbf{g}.(\mathbf{r} \times \mathbf{h})$ and $\mathbf{g} = [g(\alpha_1), g(\alpha_2), g(\alpha_3)]$. This same notation was used for the other vectors. If the lower bottom was rigid, using equations (17) - (22), the determinant can be reduced to

$$D_r = [pny][\alpha hr] + [sny][\alpha gh] + [lny][\alpha rg], \qquad (27)$$

where

$$\alpha = (\alpha_1, \alpha_2, \alpha_3), \qquad (28)$$

$$\mathbf{n} = (1, 1, 1), \qquad (29)$$

$$y(\alpha) = \alpha^2\left[\alpha^2 - 2a^2 - \dfrac{\lambda(1 + \lambda L_1)}{\sigma(1 + \lambda L_2)}\right], \qquad (30)$$

$$h(\alpha) = \lambda\left[\alpha^2 - 3a^2 - \dfrac{\lambda(1 + \lambda L_1)}{\sigma(1 + \lambda L_2)}\right]\alpha\,cosh(\alpha)$$
$$- a^2\dfrac{(1 + \lambda L_1)}{(1 + \lambda L_2)}\left(\sigma G + \dfrac{a^2}{C}\right)sinh(\alpha), \qquad (31)$$

$$l(\alpha) = \lambda\left[\alpha^2 - 3a^2 - \dfrac{\lambda(1 + \lambda L_1)}{\sigma(1 + \lambda L_2)}\right]\alpha\,sinh(\alpha)$$
$$- a^2\dfrac{(1 + \lambda L_1)}{(1 + \lambda L_2)}\left(\sigma G + \dfrac{a^2}{C}\right)cosh(\alpha), \qquad (32)$$

$$r(\alpha) = \alpha\left(\alpha^2 - a^2\right)\left[\begin{array}{c} \alpha^2 - a^2 \\ - \dfrac{\lambda(1 + \lambda L_1)}{\sigma(1 + \lambda L_2)} \end{array}\right]cosh(\alpha)$$
$$+ B_i\left\{\left(\alpha^2 - a^2\right)\left[\begin{array}{c} \alpha^2 - a^2 \\ - \dfrac{\lambda(1 + \lambda L_1)}{\sigma(1 + \lambda L_2)} \end{array}\right] - \dfrac{Ra^2(1 + Q)\dfrac{(1 + \lambda L_1)}{(1 + \lambda L_2)}}{\lambda}\right\}sinh(\alpha), \quad (33)$$

World Academy of Science, Engineering and Technology
International Journal of Mathematical and Computational Sciences
Vol:5, No:8, 2011

$$s(\alpha) = \alpha \left(\alpha^2 - a^2\right) \left[\begin{array}{c} \alpha^2 - a^2 \\ -\dfrac{\lambda(1 + \lambda L_1)}{\sigma(1 + \lambda L_2)} \end{array} \right] sinh(\alpha)$$
$$+ B_i \left\{ \left(\alpha^2 - a^2\right) \left[\begin{array}{c} \alpha^2 - a^2 \\ -\dfrac{\lambda(1 + \lambda L_1)}{\sigma(1 + \lambda L_2)} \end{array} \right] \\ -\dfrac{Ra^2(1+Q)\left(\frac{1+\lambda L_1}{1+\lambda L_2}\right)}{\lambda} \right\} cosh(\alpha),$$
$$(34)$$

$$g(\alpha) = \left\{ \begin{array}{c} \left(\alpha^2 + a^2\right) \\ +\Gamma\left(\alpha^2 - a^2\right) \left[\begin{array}{c} \alpha^2 - a^2 \\ -\frac{\lambda(1+\lambda L_1)}{\sigma(1+\lambda L_2)} \end{array} \right] \end{array} \right\} sinh(\alpha)$$
$$- \Gamma R \alpha (1+Q) \left\{ \dfrac{\left[\begin{array}{c} \alpha^2 - 3a^2 \\ -\frac{\lambda(1+\lambda L_1)}{\sigma(1+\lambda L_2)} \end{array} \right]}{\left(\sigma G + \frac{a^2}{C}\right)} \right\} cosh(\alpha), \quad (35)$$

$$p(\alpha) = \left\{ \left(\alpha^2 + a^2\right) + \Gamma\left(\alpha^2 - a^2\right) \left[\begin{array}{c} \alpha^2 - a^2 \\ -\frac{\lambda(1+\lambda L_1)}{\sigma(1+\lambda L_2)} \end{array} \right] \right\} cosh(\alpha)$$
$$- \Gamma R \alpha (1+Q) \left\{ \dfrac{\left[\alpha^2 - 3a^2 - \frac{\lambda(1+\lambda L_1)}{\sigma(1+\lambda L_2)}\right]}{\left(\sigma G + \frac{a^2}{C}\right)} \right\} sinh(\alpha).$$
$$(36)$$

The eigenvalues λ and R are then obtained by solving $D_f = 0$ or $D_r = 0$. Finally, we utilize Newton's method to to generate representative marginal curves for this problem. The critical Rayleigh number was obtained by finding the minimum R value of the corresponding marginal curves. By varying the parameters L_1, L_2, Q and observing the effect this has on the value of the critial Rayleigh number, we are able to determine the effect of the relaxation time, the retardation time, and the internal heat generation on the thermal stability of the system.

III. RESULTS AND DISCUSSION

The term that measures the degree of surface deformation is $\left(\sigma G + \frac{a^2}{C}\right)$. For simplicity, $\frac{1}{C} = 0$ is used so that the effect of surface deformation is measured only by the value of σG. Therefore as $\left(\sigma G + \frac{a^2}{C}\right) \to \infty$, it can be deduced that the surface deformation is negligible from equation (19). Since it is assumed that the surface is a very good conductor, the Biot number is also negligible in this analysis, as the thickness of the non-Newtonian fluid layer is considered to be thermally thin. It should be noted that by setting $Q = 0$, we successfully recovered the results from Ramkissoon et al. [7].

The effect of internal heat generation, Q, on the critical Rayleigh number of the Newtonian, Maxwell and Jeffrey's viscoelastic fluid is now examined for a rigid lower surface in the presence of surface deflection. Note that when $L_1 = 0 = L_2$, this is the case of a Newtonian fluid layer. When $L_2 = 0$ but L_1 is not zero, we are considering a Maxwell viscoelastic fluid layer, and when both L_1 but L_2 are non-zero, we are considering a Jeffreys' viscoelastic fluid layer.
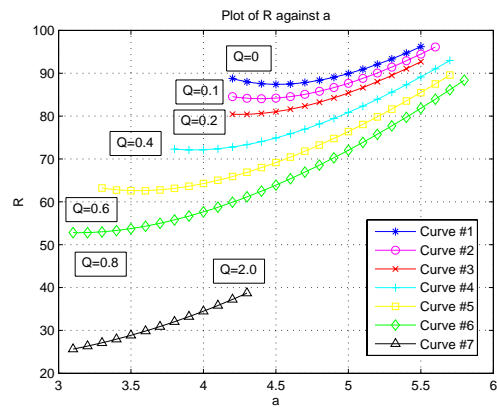

Fig. 1. Marginal stability curves for a Newtonian fluid for a rigid lower surface in the presence of surface deflection and internal heat generation. Set $L_1 = L_2 = 0$, $\sigma = 1$, $G = 150$ and $\Gamma = 1.8$ and vary Q
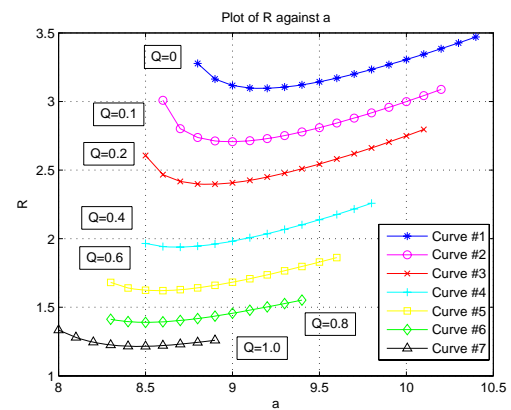

Fig. 2. Marginal stability curves for a Maxwell fluid for a rigid lower surface in the presence of surface deflection and internal heat generation. Set $L_1 = 0.5$, $L_2 = 0$, $\sigma = 1$, $G = 150$ and $\Gamma = 1.8$ and vary Q.

From figure 1, Q has a destabilizing effect because as internal heat generation was introduced into the problem, (i.e. as Q increased) the critical Rayleigh number decreased. The critical Rayleigh number in the absence of internal heat generation when $Q = 0$ (represented by Curve #1 in Figure 1) is 87.399473. This value continuously decreased from 84.047585 when $Q = 0.1$ (in Curve #2) to 80.413782 for $Q = 0.2$ (in Curve #3) to 72.095834 for $Q = 0.4$ (in Curve #4) to 62.561497 for $Q = 0.6$ (in Curve #5) to 52.794642 for $Q = 0.8$ (in Curve #6) and to a much lower value when Q is increased to 2.0 (in Curve #7). Therefore Q has a destabilizing effect for the Newtonian fluid.

Next, the effect of Q on a Maxwell viscoelastic fluid layer is examined. From figure 2, we see that Q had a destabilizing effect on the Maxwell fluid because as internal heat generation is introduced into the problem, (i.e. as Q increased) the critical Rayleigh number decreases. The critical Rayleigh number in the absence of internal heat generation when $Q = 0$ (represented by Curve #1 in figure 1) is 3.095966. This value continuously decreases from 2.706709 when $Q = 0.1$ (in

World Academy of Science, Engineering and Technology
International Journal of Mathematical and Computational Sciences
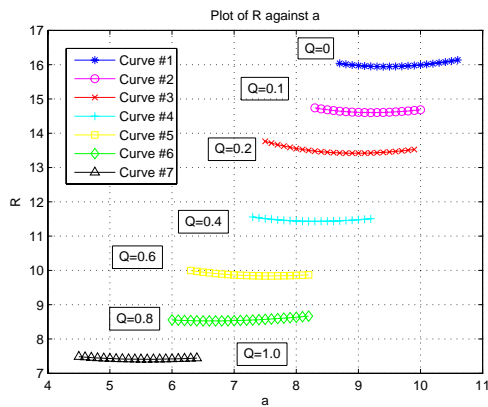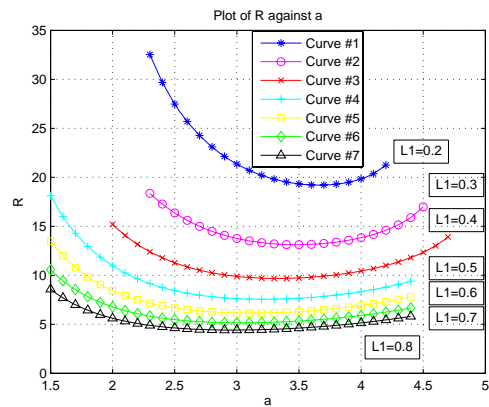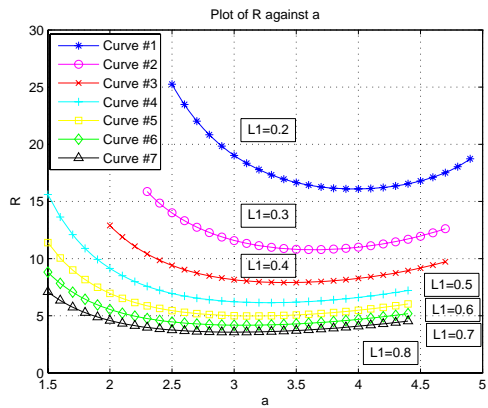Vol:5, No:8, 2011

Fig. 3. Marginal stability curves for a Jeffrey's viscoelastic fluid for a rigid lower surface in the presence of surface deflection and internal heat generation. Set $L_1 = 0.2$, $L_2 = 0.02$ $\sigma = 1$, $G = 150$ and $\Gamma = 1.8$ and vary Q.

Fig. 4. Marginal stability curves for a Maxwell fluid for a rigid lower surface in the presence of surface deflection and absence of internal heat generation for various values of L_1. Set $L_2 = 0$, $\sigma = 1$, $G = 150$ $Q = 0$ and $\Gamma = 1.8$ and vary L_1.

Curve #2) to 2.397482 for $Q = 0.2$ (in Curve #3) to 1.938646 for $Q = 0.4$ (in Curve #4) to 1.621464 for $Q = 0.6$ (in Curve #5) to 1.390132 for $Q = 0.8$ (in Curve #6) and even lower to 1.215720 when $Q = 1.0$ (in Curve #7).

We now examine the effect of Q on the Jeffreys' viscoelastic fluid. From figure 3, Q also has a destabilizing effect for the Jeffrey's viscoelastic fluid because as internal heat generation is introduced into the problem, (i.e. as Q increased) the critical Rayleigh number decreases. The critical Rayleigh number in the absence of internal heat generation when $Q = 0$ (represented by Curve #1 in figure 1) is 15.941500. This value continuously decreased from 14.601399 when $Q = 0.1$ (in Curve #2) to 13.416766 for $Q = 0.2$ (in Curve #3) to 11.431372 for $Q = 0.4$ (in Curve #4) to 9.839724 for $Q = 0.6$ (in Curve #5) to 8.527079 for $Q = 0.8$ (in Curve #6) and even lower to 7.408198 when $Q = 1.0$ (in Curve #7).

Next, the effect of varying L_1 of a Maxwell fluid in the absence and presence of internal heat generation is examined. From figure 4, L_1 has a destabilizing effect on the Maxwell fluid in the absence of internal heat generation because as L_1

increases the critical Rayleigh number decreases for $Q = 0$. The critical Rayleigh number when $L_1 = 0.2$ is 16.153435 and this value continuously decreases to 10.789833 when $L_1 = 0.3$ (in Curve #2) to 7.899738 for $L_1 = 0.4$ (in Curve #3) to 6.143143 for $L_1 = 0.5$ (in Curve #4) to 4.983025 for $L_1 = 0.6$ (in Curve #5) to 4.166746 for $L_1 = 0.7$ (in Curve #6) and even lower to 3.565803 when $L_1 = 0.8$ (in Curve #7).

The effect of L_1 on the Maxwell fluid in the presence of internal heat generation is now examined. From figure 5, L_1 also has a destabilizing effect on the Maxwell fluid in the presence of internal heat generation because as L_1 increased the critical Rayleigh number decreases for $Q = 0.2$. The critical Rayleigh number when $L_1 = 0.2$ is 19.215832 and this value continuously decreases to 13.121989 when $L_1 = 0.3$ (in Curve #2) to 9.677033 for $L_1 = 0.4$ (in Curve #3) to 7.553862 for $L_1 = 0.5$ (in Curve #4) to 6.142501 for $L_1 = 0.6$ (in Curve #5) to 5.147448 for $L_1 = 0.7$ (in Curve #6) and even lower to 4.412003 when $L_1 = 0.8$ (in Curve #7). Therefore the non-dimensional relaxation time, L_1, has a destabilizing effect on the Maxwell fluid both in the absence and presence of internal heat generation.

Next, the effect of varying L_1 and L_2 of a Jeffreys' viscoelastic fluid in the absence and presence of internal heat is examined. We see from figure 6 that L_1 has a destabilizing effect on the Jeffreys' viscoelastic fluid in the absence of internal heat generation because as L_1 increases the critical Rayleigh number decreases for $Q = 0$. The critical Rayleigh number when $L_1 = 0.2$ is 15.941499 and this value continuously decreases to 13.063460 when $L_1 = 0.25$ (in Curve #2) to 11.157836 for $L_1 = 0.3$ (in Curve #3) to 9.794140 for $L_1 = 0.35$ (in Curve #4) and even lower to 8.765256 when $L_1 = 0.4$ (in Curve #5). Therefore L_1 has a destabilizing effect on the Jeffrey's viscoelastic fluid in the absence of internal heat generation.

From figure 7, L_1 has a destabilizing effect on the Jeffrey's viscoelastic fluid in the presence of internal heat generation because as L_1 increases the critical Rayleigh number decreases when $Q = 0.6$. The critical Rayleigh number when $L_1 = 0.2$

World Academy of Science, Engineering and Technology
International Journal of Mathematical and Computational Sciences
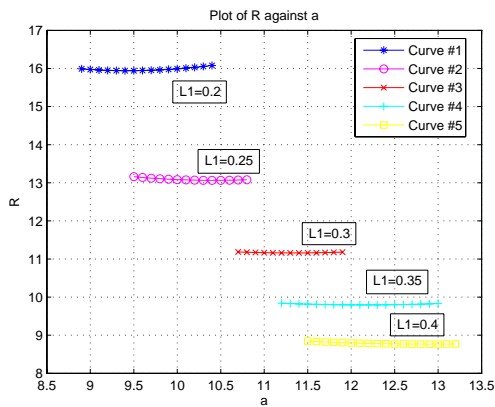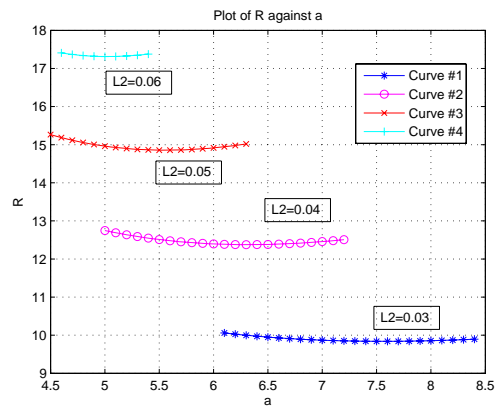Vol:5, No:8, 2011

Fig. 6. Marginal stability curves for a Jeffreys' viscoelastic fluid for a rigid lower surface in the presence of surface deflection and absence of internal heat for various values of L_1. Set $L_2 = 0.02$, $\sigma = 1$, $G = 150$ $Q = 0$ and $\Gamma = 1.8$ and vary L_1.

Fig. 8. Marginal stability curves for a Jeffreys' viscoelastic fluid for a rigid lower surface in the presence of surface deflection and internal heat generation, $Q = 0.6$, for various values of L_2. Set $L_1 = 0.02$, $\sigma = 1$, $G = 150$ $Q = 0.6$ and $\Gamma = 1.8$ and vary L_2.
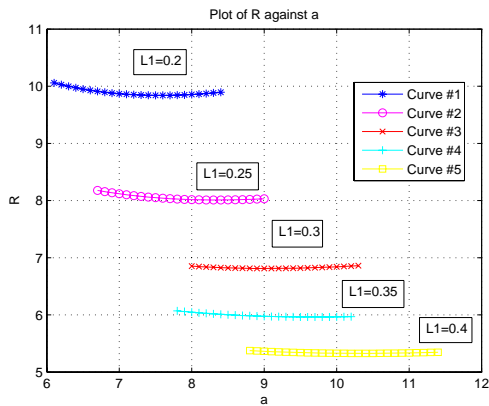

Fig. 7. Marginal stability curves for oscillations in a Jeffreys' viscoelastic fluid for a rigid lower surface in the presence of surface deflection and internal heat, $Q = 0.6$, for various values of L_1. Set $L_2 = 0.02$, $\sigma = 1$, $G = 150$ $Q = 0.6$ and $\Gamma = 1.8$ and vary L_1.
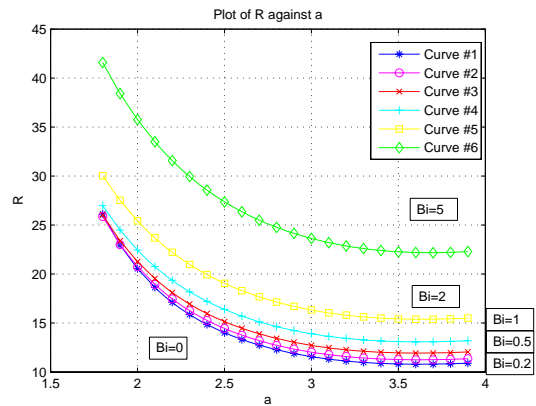

Fig. 9. Marginal stability curves for a Maxwell fluid with a rigid lower surface in the presence of surface deflection and absence of internal heat generation for various values of B_i. Set $L_1 = 0.3$, $\sigma = 1$, $G = 150$ $Q = 0$ and $\Gamma = 1.8$ and vary B_i.

(in Curve #1) was 9.839724 and this value continuously decreases to 8.009679 when $L_1 = 0.25$ (in Curve #2) to 6.811227 for $L_1 = 0.3$ (in Curve #3) to 5.962055 for $L_1 = 0.35$ (in Curve #4) and even lower to 5.326499 when $L_1 = 0.4$ (in Curve #5). Therefore the non dimensional relaxation time, L_1, is destabilizing for the Jeffrey's viscoelastic fluid both in the absence and presence of internal heat generation.

The stabilizing effect of varying L_2 for a Jeffrey's viscoelastic fluid in the absence of internal heat generation was examined by Ramkissoon et al. [7]. We now study the effect of varying L_2 of a Jeffrey's viscoelastic fluid in the presence of internal heat generation.

From figure 8, L_2 also had a stabilizing effect on the Jeffreys' viscoelastic fluid in the presence of internal heat generation because as L_2 increases the critical Rayleigh number increases for $Q = 0.6$. The critical Rayleigh number when $L_2 = 0.03$ was 9.839724 and this value continuously increases to 12.376017 when $L_2 = 0.04$ (in Curve #2) to 14.856154 for $L_2 = 0.05$ (in Curve #3) and even higher to 17.313016 when

$L_2 = 0.06$ (in Curve #4). Therefore L_2 has a stabilizing effect on the Jeffrey's viscoelastic fluid in the presence of internal heat generation. Therefore, the non-dimensional retardation time, L_2, is stabilizing for the Jeffrey's viscoelastic fluid both in the absence and presence of internal heat generation.

Finally, the effect of the biot number, B_i, on the Maxwell and Jeffrey's viscoelastic fluid is examined both in the absence and presence of internal heat generation. From figure 9, B_i has a stabilizing effect on the Maxwell fluid in the absence of internal heat generation because as B_i is increased the critical Rayleigh number increases for $Q = 0$. The critical Rayleigh number when $B_i = 0$ is 10.789833 and this value continuously increases to 11.242480 when $B_i = 0.2$ (in Curve #2) to 11.926157 for $B_i = 0.5$ (in Curve #3) to 13.073684 for $B_i = 1$ (in Curve #4) to 15.378891 for $B_i = 2$ (in Curve #5) and even higher to 22.169618 when $B_i = 5$ (in Curve #6). Therefore B_i has a stabilizing effect on the Maxwell fluid in the absence of internal heat generation.

From figure 10, B_i has a stabilizing effect on the Maxwell

World Academy of Science, Engineering and Technology
International Journal of Mathematical and Computational Sciences
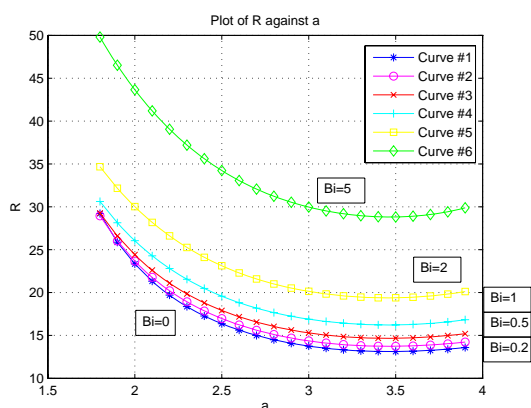Vol:5, No:8, 2011

Fig. 10. Marginal stability curves for a Maxwell fluid with a rigid lower surface in the presence of surface deflection and presence of internal heat generation for various values of B_i. Set $L_1 = 0.3$, $\sigma = 1$, $G = 150$ $Q = 0.2$ and $\Gamma = 1.8$ and vary B_i.
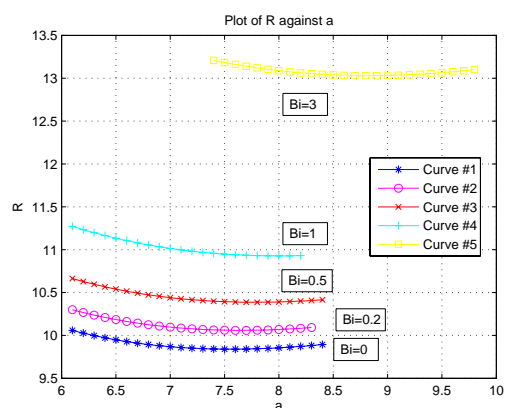

Fig. 12. Marginal stability curves for a Jeffreys' viscoelastic fluid for a rigid lower surface in the presence of surface deflection and presence of internal heat generation for various values of B_i. Set $L_1 = 0.2$, $L_2 = 0.02$, $\sigma = 1$, $G = 150$ $Q = 0.6$ and $\Gamma = 1.8$ and vary B_i.

the Jeffreys' viscoelastic fluid in the absence of internal heat generation.

Figure 12 illustrates that B_i has a stabilizing effect on a Jeffreys' viscoelastic fluid layer in the presence of internal heat generation, because as B_i is increased, the critical Rayleigh number increases for $Q = 0.6$. The critical Rayleigh number when $B_i = 0$ is 9.839724 and this value continuously increases to 10.059360 when $B_i = 0.2$ (in Curve #2) to 10.386719 for $B_i = 0.5$ (in Curve #3) to 10.927610 for $B_i = 1$ (in Curve #4) and even higher to 13.029142 when $B_i = 3$ (in Curve #5). Therefore, the biot number, B_i, is stabilizing for the Jeffreys' viscoelastic fluid both in the absence and presence of internal heat generation.
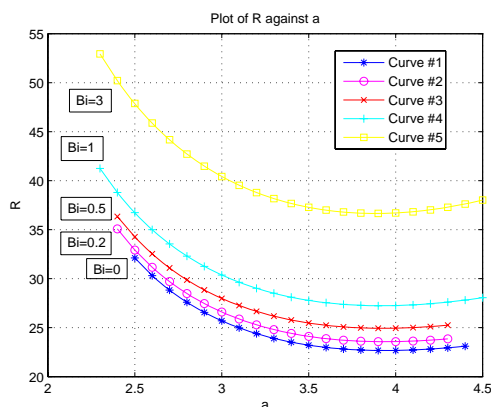

Fig. 11. Marginal stability curves for a Jeffreys' viscoelastic fluid with a rigid lower surface in the presence of surface deflection and absence of internal heat generation for various values of B_i. Set $L_1 = 0.2$, $L_2 = 0.02$, $\sigma = 1$, $G = 150$ $Q = 0$ and $\Gamma = 1.8$ and vary B_i.

IV. CONCLUSION

For the Bénard-Marangoni problem investigating the onset of overstability in a viscoelastic Jeffrey's fluid layer subjected to internal heat generation, the presence of internal heat generation, Q, has a destabilizing effect for the Newtonian, Maxwell and Jeffrey's viscoelastic fluid which is enhanced as Q is increased. The non-dimensional relaxation time, L_1, has a destabilizing effect on both the Maxwell and Jeffrey's viscoelastic fluid both in the absence and presence of internal heat generation. The non-dimensional retardation time, L_2, is stabilizing for the Jeffrey's viscoelastic fluid both in the absence and presence of internal heat generation. Also, the biot number, B_i, is stabilizing for the Maxwell and Jeffrey's viscoelastic fluid both in the absence and presence of internal heat generation.

fluid in the presence of internal heat generation because as B_i is increased, the critical Rayleigh number increases for $Q = 0.2$. The critical Rayleigh number when $B_i = 0$ is 13.121989 and this value continuously increases to 13.736120 when $B_i = 0.2$ (in Curve #2) to 14.665542 for $B_i = 0.5$ (in Curve #3) to 16.230288 for $B_i = 1$ (in Curve #4) to 19.389672 for $B_i = 2$ (in Curve #5) and even higher to 28.818018 when $B_i = 5$ (in Curve #6). Therefore, the biot number, B_i, is stabilizing for the Maxwell fluid both in the absence and presence of internal heat generation.

We see from figure 9 that B_i has a stabilizing effect on the Jeffrey's viscoelastic fluid in the absence of internal heat generation because as B_i is increased, the critical Rayleigh number increases for $Q = 0$. The critical Rayleigh number when $B_i = 0$ is 22.670500 and this value continuously increases to 23.570304 when $B_i = 0.2$ (in Curve #2) to 24.933907 for $B_i = 0.5$ (in Curve #3) to 27.236250 for $B_i = 1$ (in Curve #4) and even higher to 36.656678 for $B_i = 3$ (in Curve #5). Therefore B_i has a stabilizing effect on

REFERENCES

[1] H. Benard. Les tourbillons cellularies dans une nappe liquid. *Revus Generale Des Sciences Pures Et Appliqus*, 11:1261–1271, 1900.
[2] Lord Rayleigh. On the convection currents in a horizontal layer of fluid when the higher temperature is on the underside. *Phil. Mag.*, 32:529–546, 1916.
[3] J. R. A. Pearson. On convection cells induced by surface tension. *J. Fluid Mech.*, 4:489–500, 1958.
[4] D. A. Nield. Surface tension and buoyancy effects in cellular convection. *J. Fluid Mech.*, 19:341–352, 1964.

World Academy of Science, Engineering and Technology
International Journal of Mathematical and Computational Sciences
Vol:5, No:8, 2011

[5] R. D. Benguria and M. C. Depassier. On the linear stability theory of bnard-marangoni convection. *Phys. Fluids A1*, 7:1123–1127, 1989.

[6] C. Perez-Garcia and G. Carneiro. Linear stability analysis of bnard-marangoni convection in fluids with a deformable surface. *Phys. Fluids A3*, 2:292–298, 1991.

[7] H. Ramkissoon, G. Ramdath, D. M. G. Comissiong, and K. Rahaman. On thermal instabilities in a viscoelastic fluid. *J. Non-Linear Mech.*, 41:18–25, 2006.

[8] E. M. R. Sparrow, R. J. Goldstein, and V. K. Johnson. Thermal instability on a horizontal fluid layer: Effect of boundary conditions and non-linear temperature profile. *J. Fluid Mech.*, 18:513–529, 1964.

[9] P. H. Roberts. Convection in horizontal layers with internal heat generation: Theory. *J. Fluid Mech.*, 30:33–49, 1967.

[10] P. D. Gasser and M. S. Kazimi. Onset of convection in a porous medium with internal heat generation. *J. Heat Transfer*, 98:49–54, 1976.

[11] M. Kaviany. Thermal convection instabilities in a porous medium. *J. Heat Transfer*, 106:137–142, 1984.

[12] M. Char and K. Chiang. Stability analysis of benard-marangoni convection in fluids with internal heat generation. *J. of Physics D: Applied Physics*, 27:748–755, 1994.

[13] M. Char, K. Chiang, and J. Jou. Oscillatory instability analysis of benard-marangoni convection in a rotating fluid with internal heat generation. *Int. J. Heat Mass Transfer*, 40:857–867, 1997.

[14] I. Hashim, H. Othman, and S. A. Kechil. Stabilization of thermocapillary instability in a fluid layer with internal heat source. *Int. Comm. Heat Mass Transfer*, 36(2):161–165, 2009.

[15] C. E. Nanjundappa, I. S. Shivakumara, J. Lee, and M. Ravisha. Effect of internal heat generation on the onset of brinkman-benard convection in a ferrofluid saturated porous layer. *Int. J. of Thermal Sci.*, 50(2):160–168, 2011.

[16] K. Abdul, A. Mohammed, and S. Sharidan. Free convection boundary layer flow of a viscoelastic fluid in the presence of heat generation. *World Academy of Sci. Engng. and Tech.*, 75:492–499, 2011.